

Fig. 1 Schematic representations of (a) overall construction of Flow Boiling Module (FBM), (b) construction of heating slabs, and (c) substrate temperature measurement.

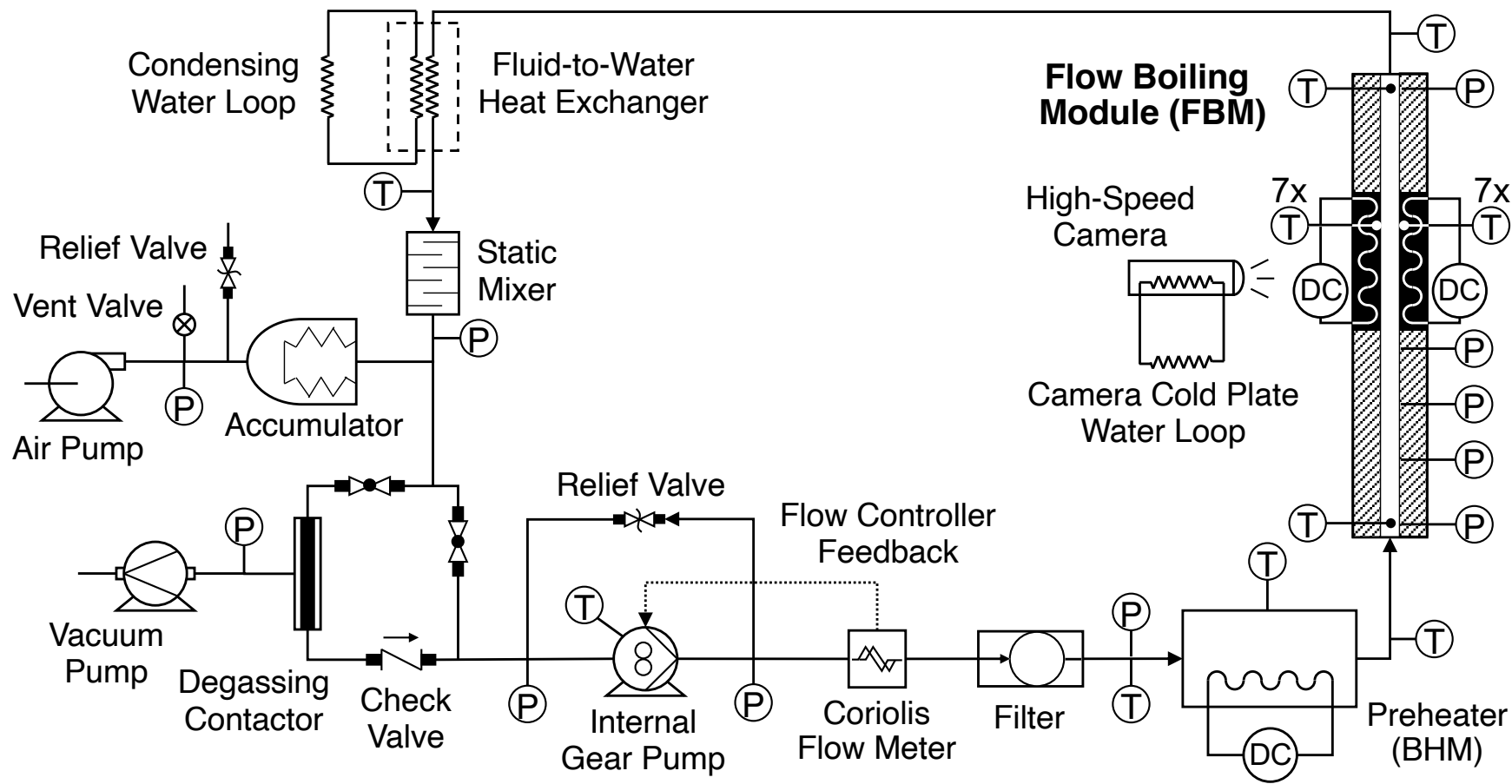


Fig. 2 Schematic diagram of experimental two-phase flow loop.

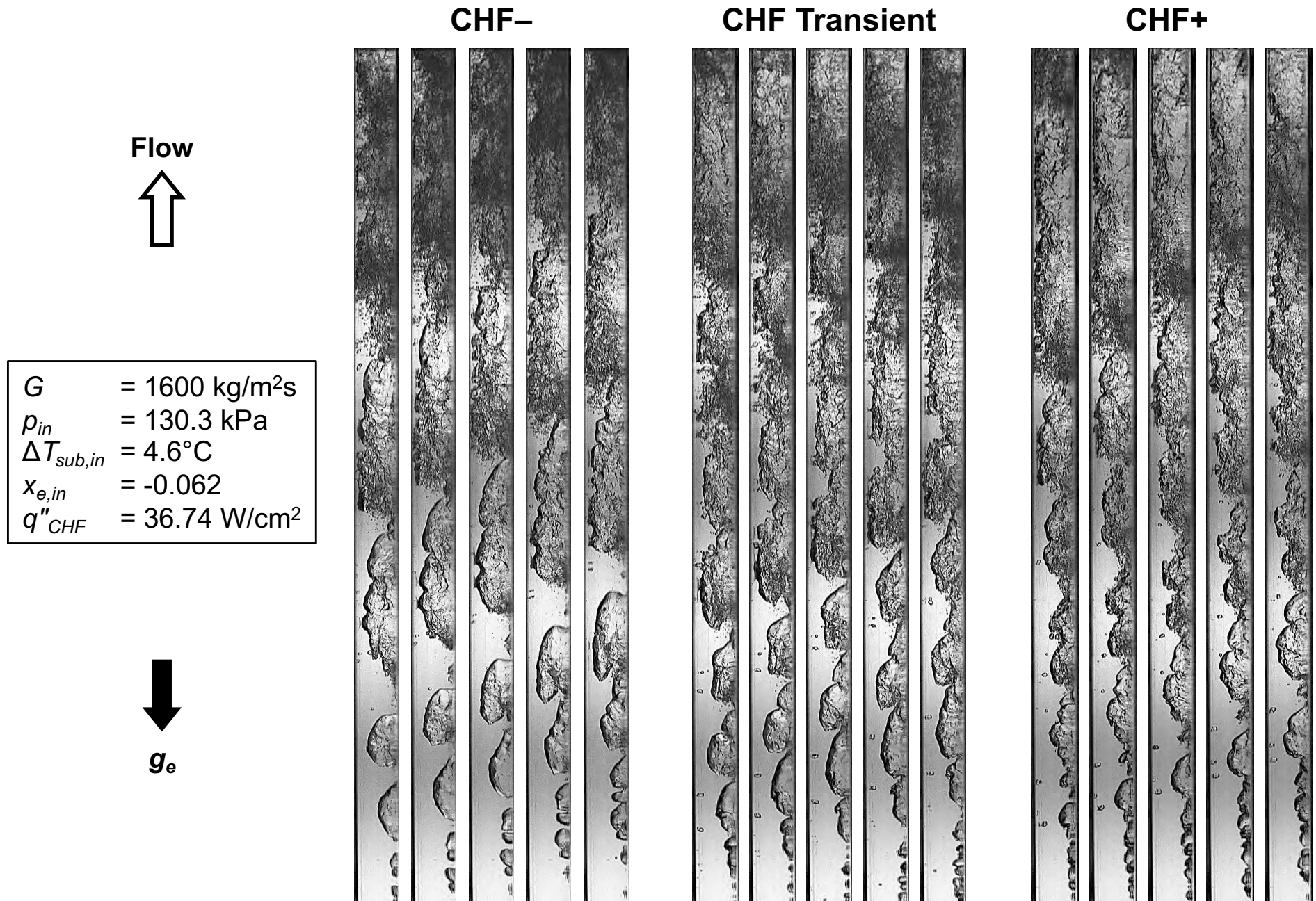


Fig. 3 Sequential images during CHF-, CHF transient, and CHF+ for $G = 1600 \text{ kg/m}^2\text{s}$, $p_{in} = 130.3 \text{ kPa}$, $\Delta T_{sub,in} = 4.6^\circ\text{C}$, $x_{e,in} = -0.062$, and $q''_{CHF} = 36.74 \text{ W/cm}^2$ with single-sided heating. The interval between successive images in all sequences is 1.5 ms.

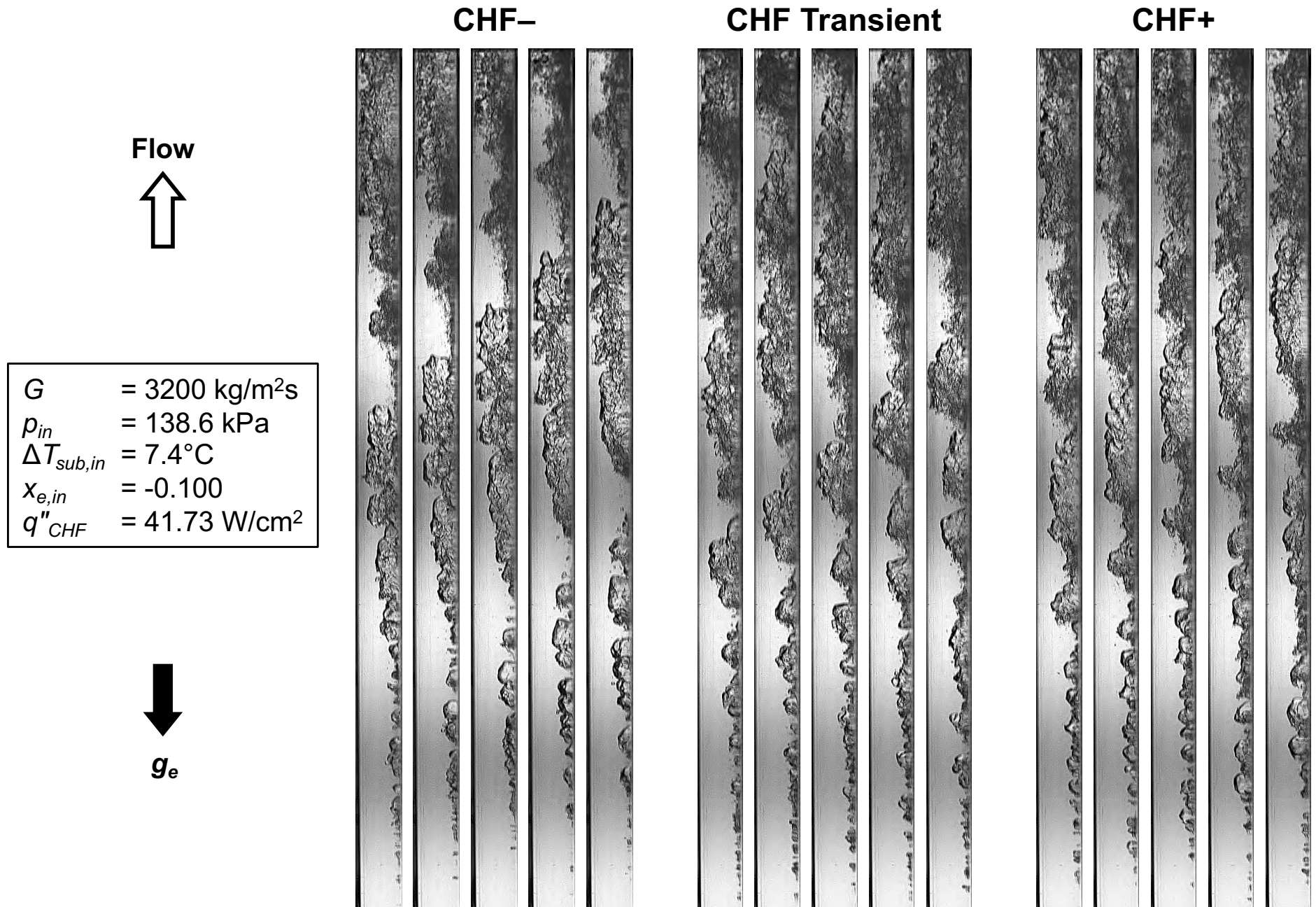


Fig. 4 Sequential images during CHF-, CHF transient, and CHF+ for $G = 3200 \text{ kg/m}^2\text{s}$, $p_{in} = 138.6 \text{ kPa}$, $\Delta T_{sub,in} = 7.4^\circ\text{C}$, $x_{e,in} = -0.100$, and $q''_{CHF} = 41.73 \text{ W/cm}^2$ with single-sided heating. The interval between successive images in all sequences is 1.5 ms.

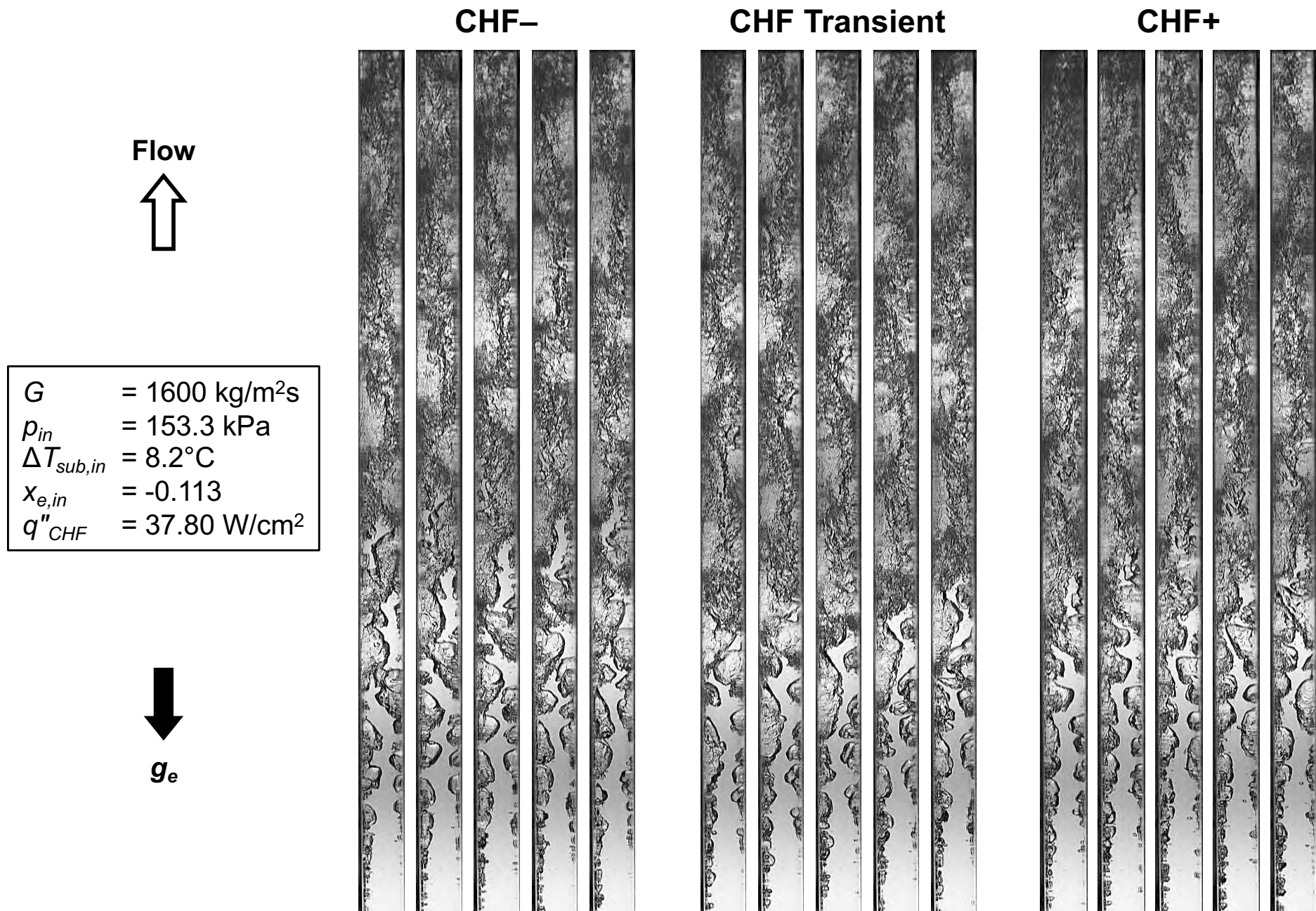


Fig. 5 Sequential images during CHF-, CHF transient, and CHF+ for $G = 1600 \text{ kg/m}^2\text{s}$, $p_{in} = 153.3 \text{ kPa}$, $\Delta T_{sub,in} = 8.2^\circ\text{C}$, $x_{e,in} = -0.113$, and $q''_{CHF} = 37.80 \text{ W/cm}^2$ with double-sided heating. The interval between successive images in all sequences is 1.5 ms.

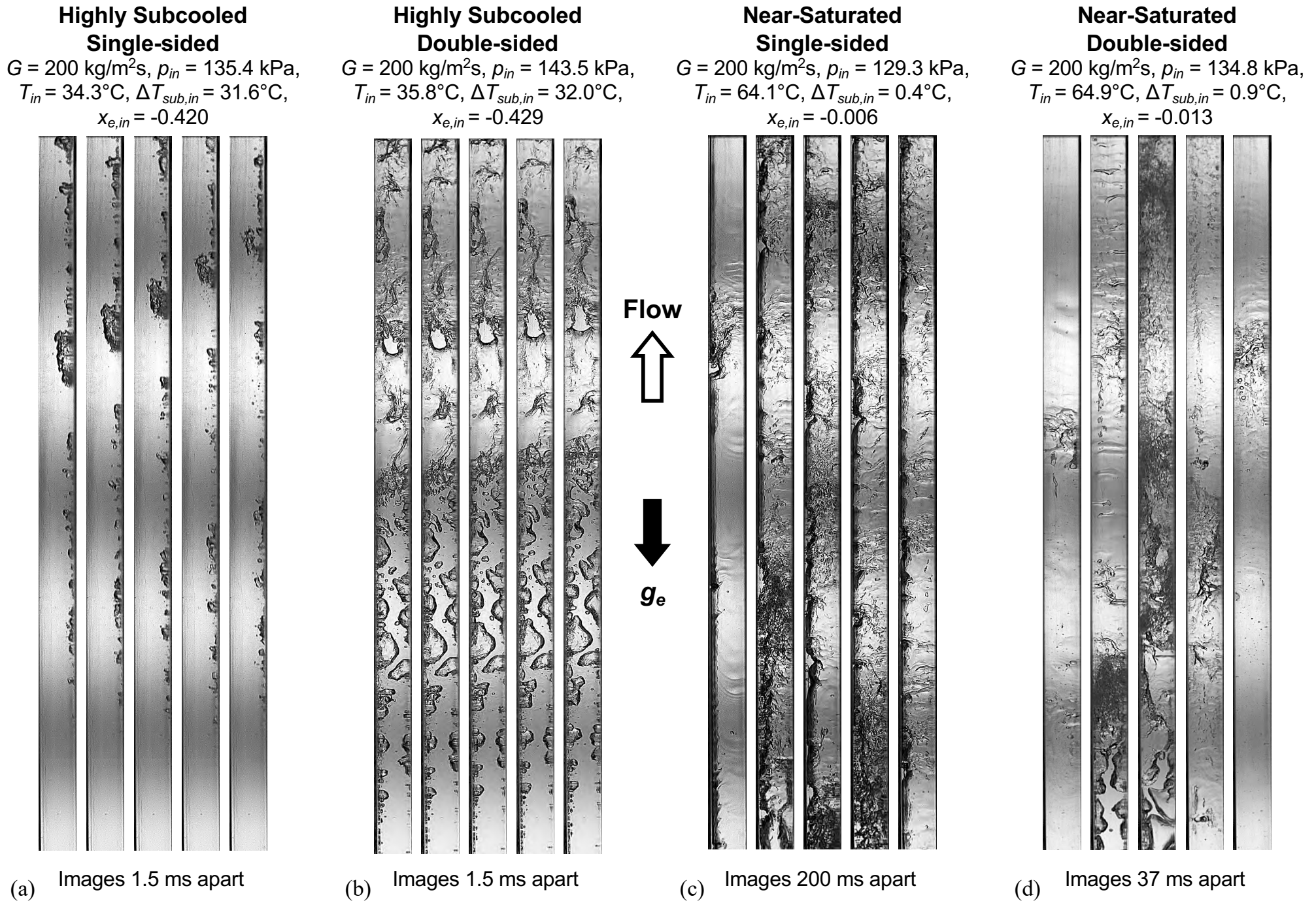
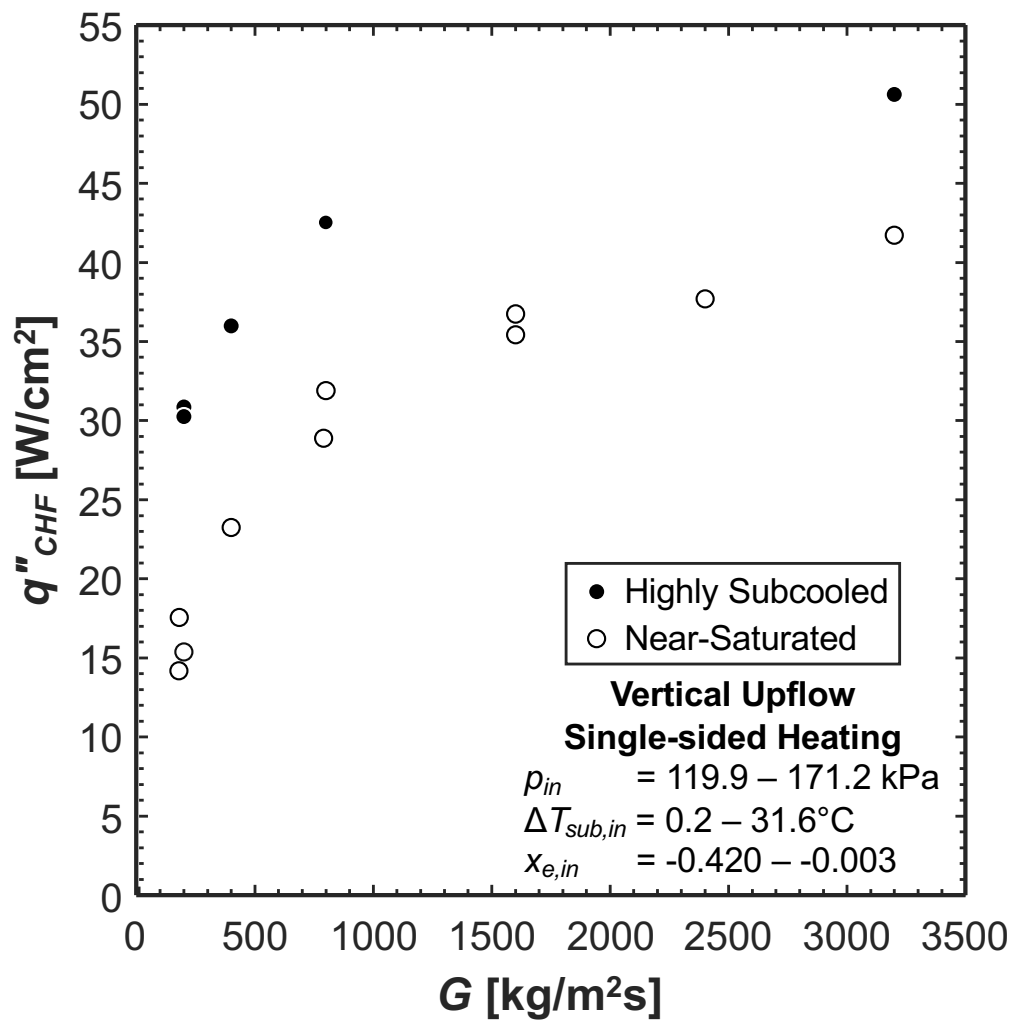
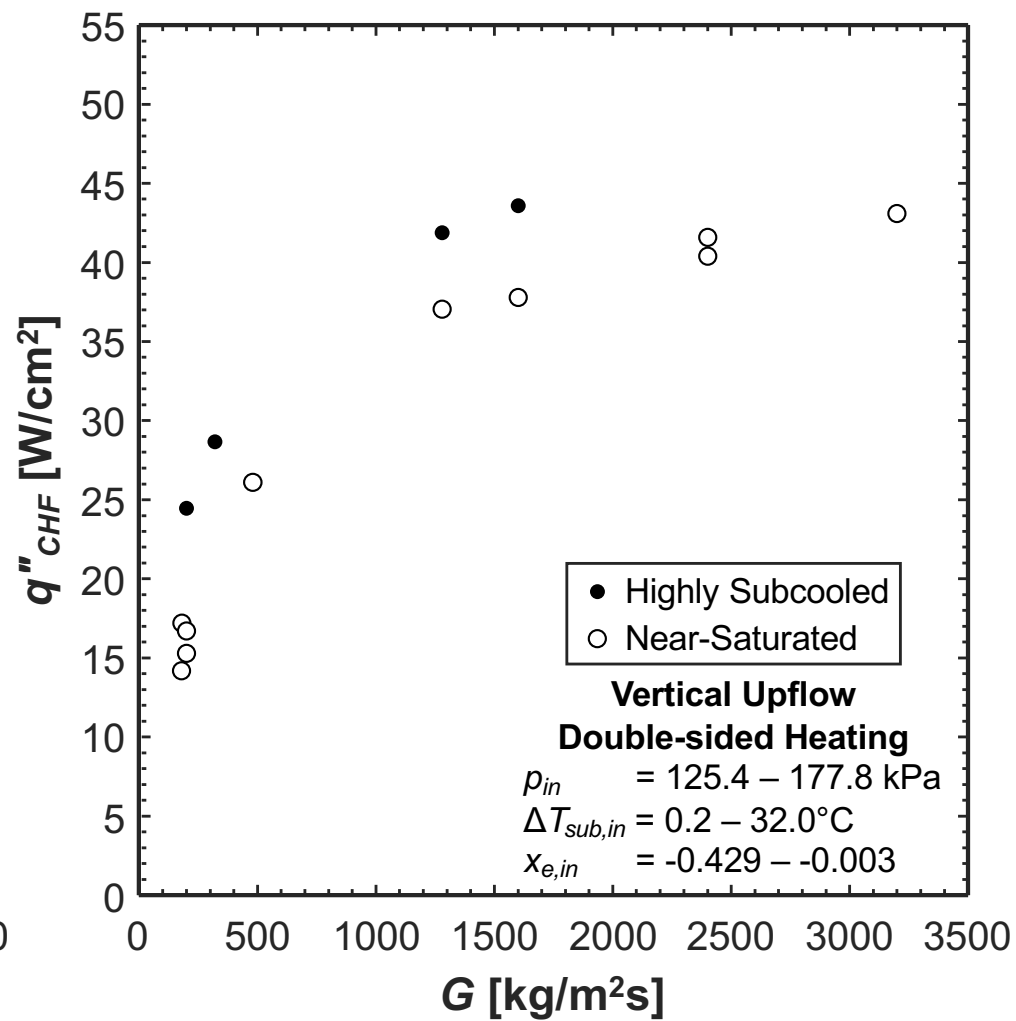


Fig. 6 Sequential images of CHF transient for $G = 200 \text{ kg/m}^2\text{s}$ and heating configurations of a) highly subcooled single-sided, b) highly subcooled double-sided, c) near-saturated single-sided, and d) near-saturated double sided. Time interval between successive images is indicated below each sequence.

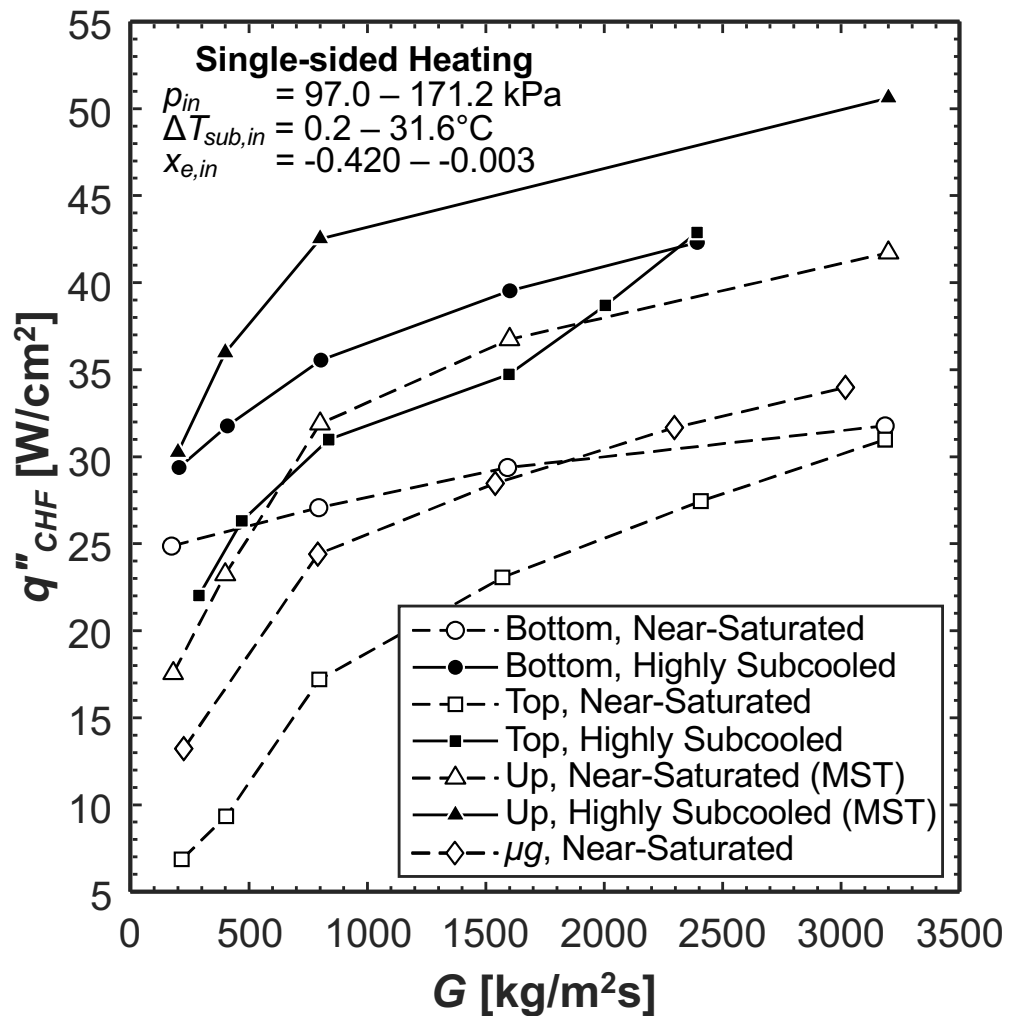


(a)

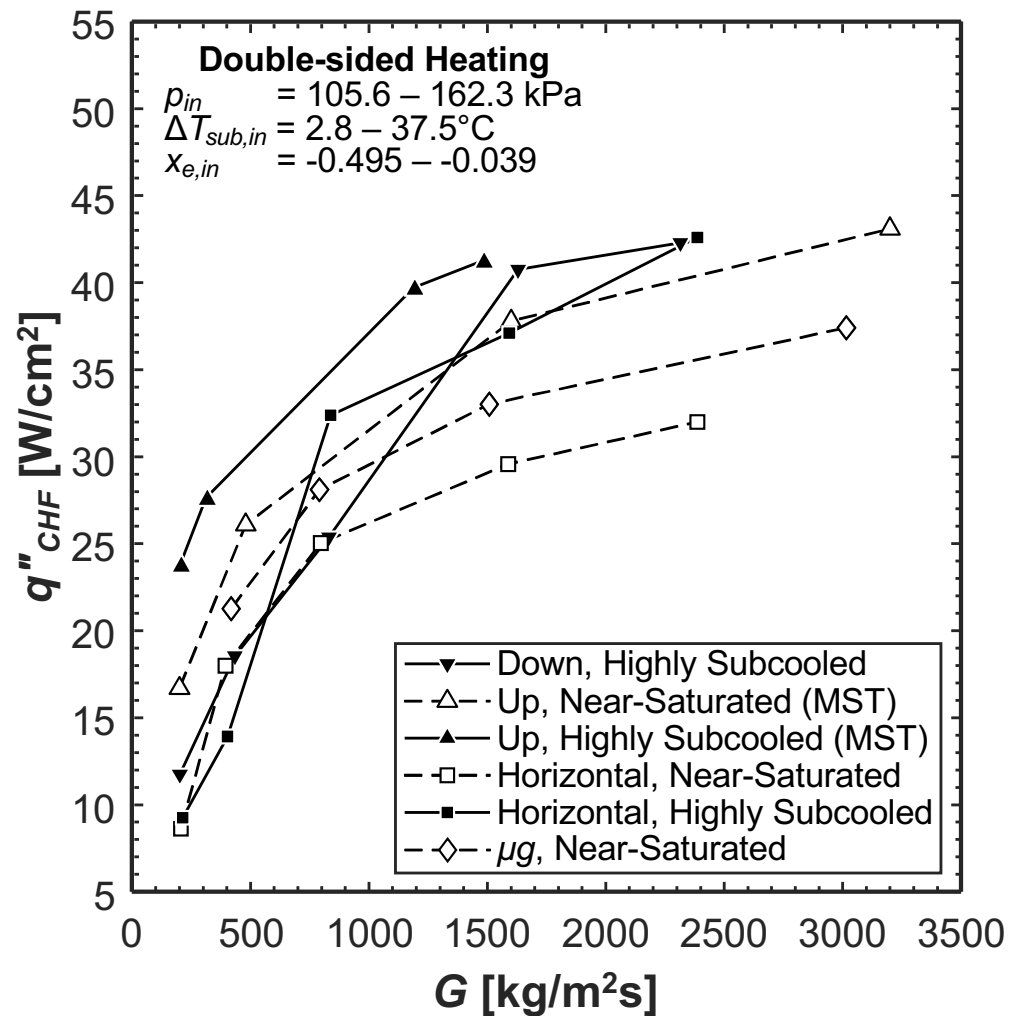


(b)

Fig. 7 MST Experimental CHF results for (a) single-sided heating and (b) double sided heating.



(a)



(b)

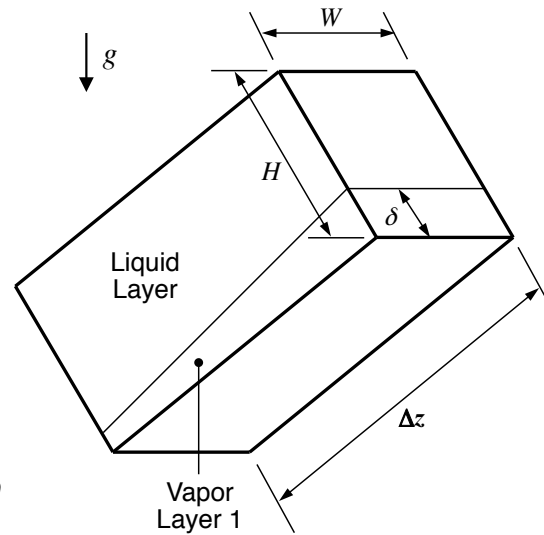
Fig. 8 Experimental CHF results for a subset of the consolidated database for (a) single-sided heating and (b) double sided heating.

Single-sided Heating

$$A_g = \delta W$$

$$A_f = (H - \delta)W$$

Control Volumes of Length Δz



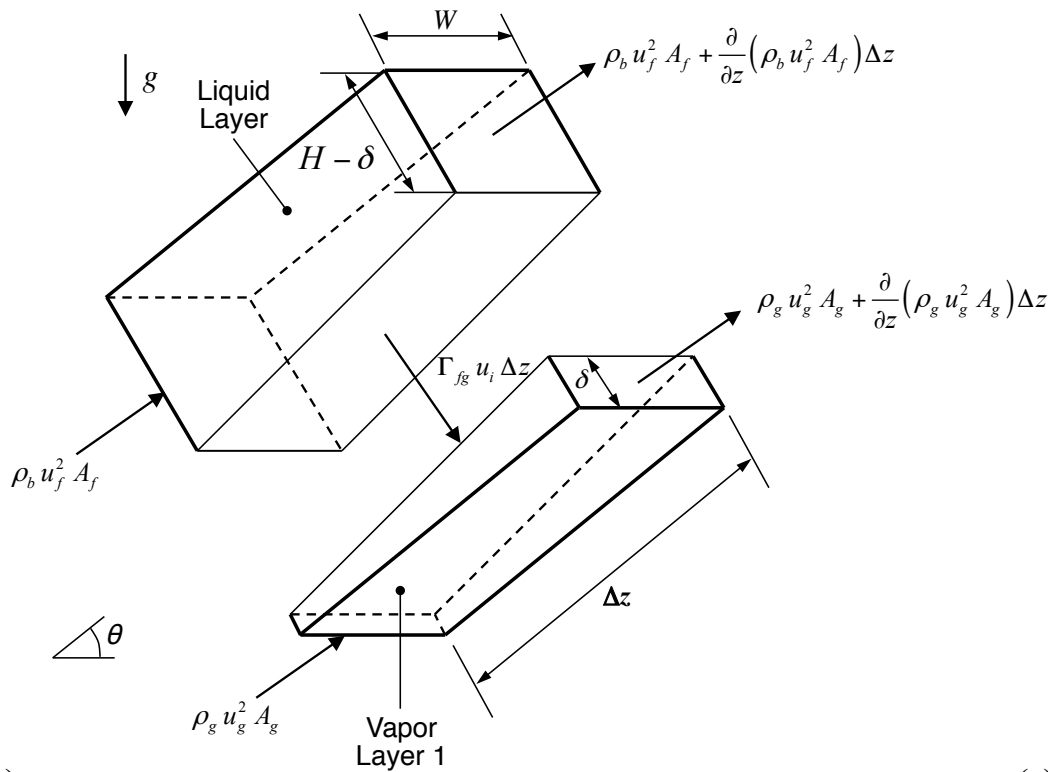
$$P_{w,g} = W + 2\delta$$

$$P_{w,f} = 2(H - \delta)$$

$$P_i = W$$

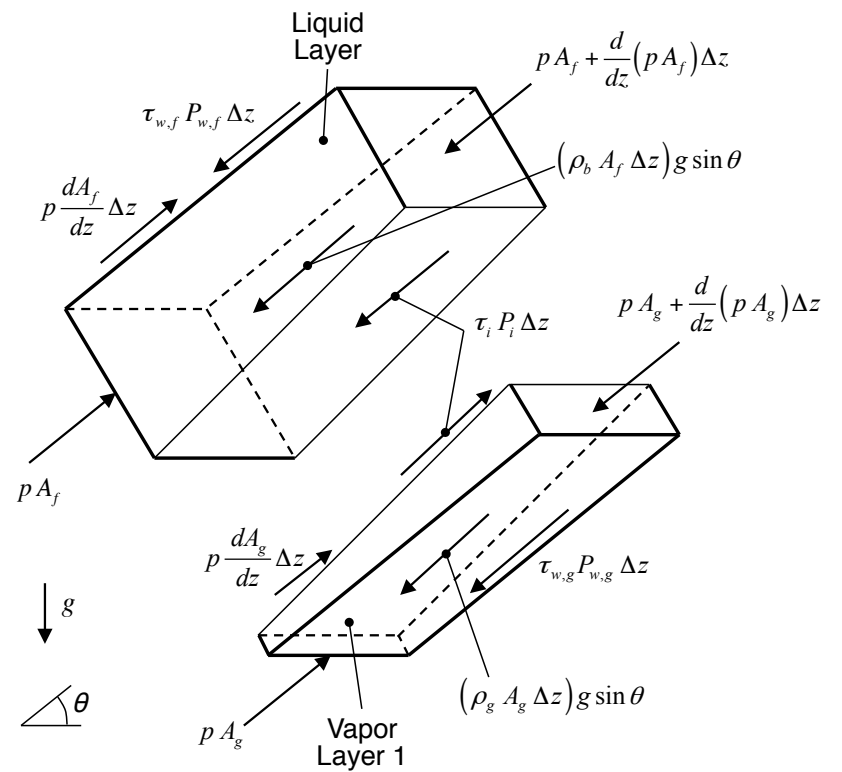
(a)

Momentum Conservation Terms



(b)

Force Conservation Terms



(c)

Fig. 9 Separated flow modelling of single-sided heating configuration: (a) control volumes of length Δz , (b) momentum terms for individual layers, and (c) force terms for individual layers.

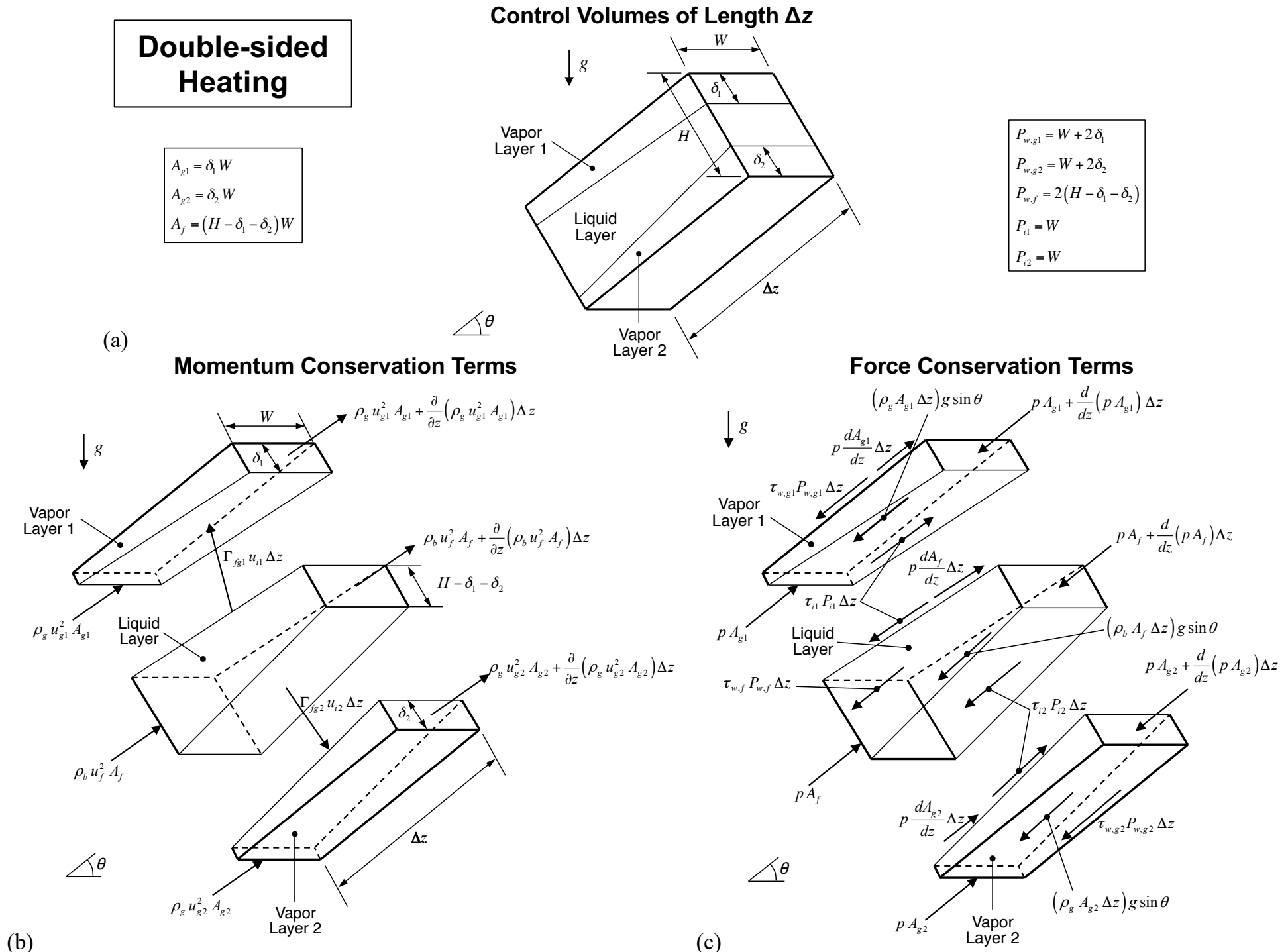
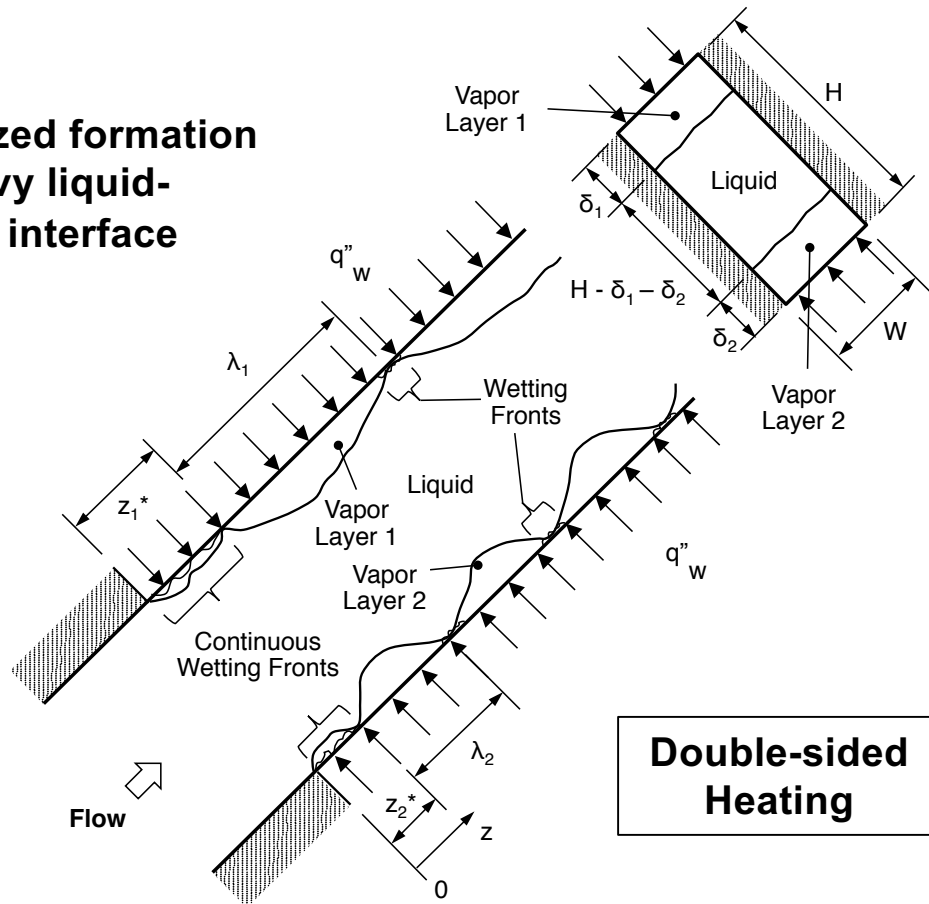


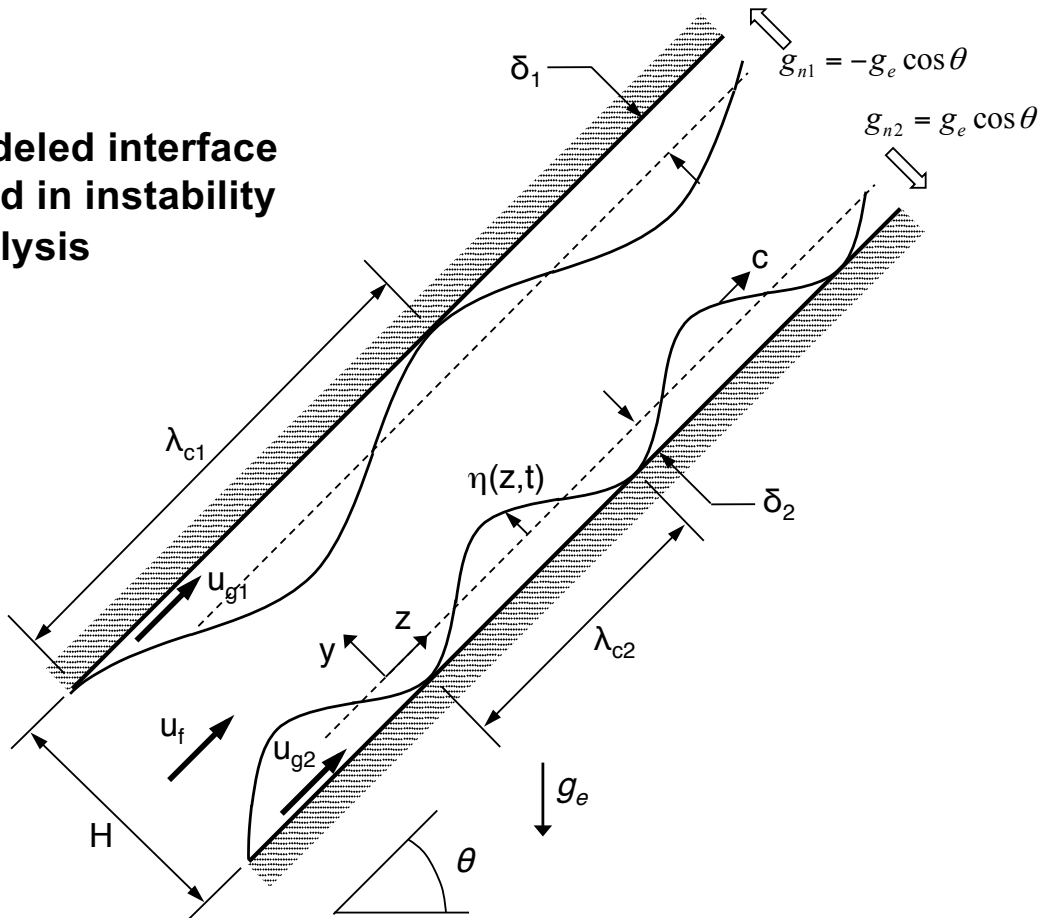
Fig. 10 Separated flow modelling of double-sided heating configuration: (a) control volumes of length Δz , (b) momentum terms for individual layers, and (c) force terms for individual layers.

Idealized formation of wavy liquid-vapor interface



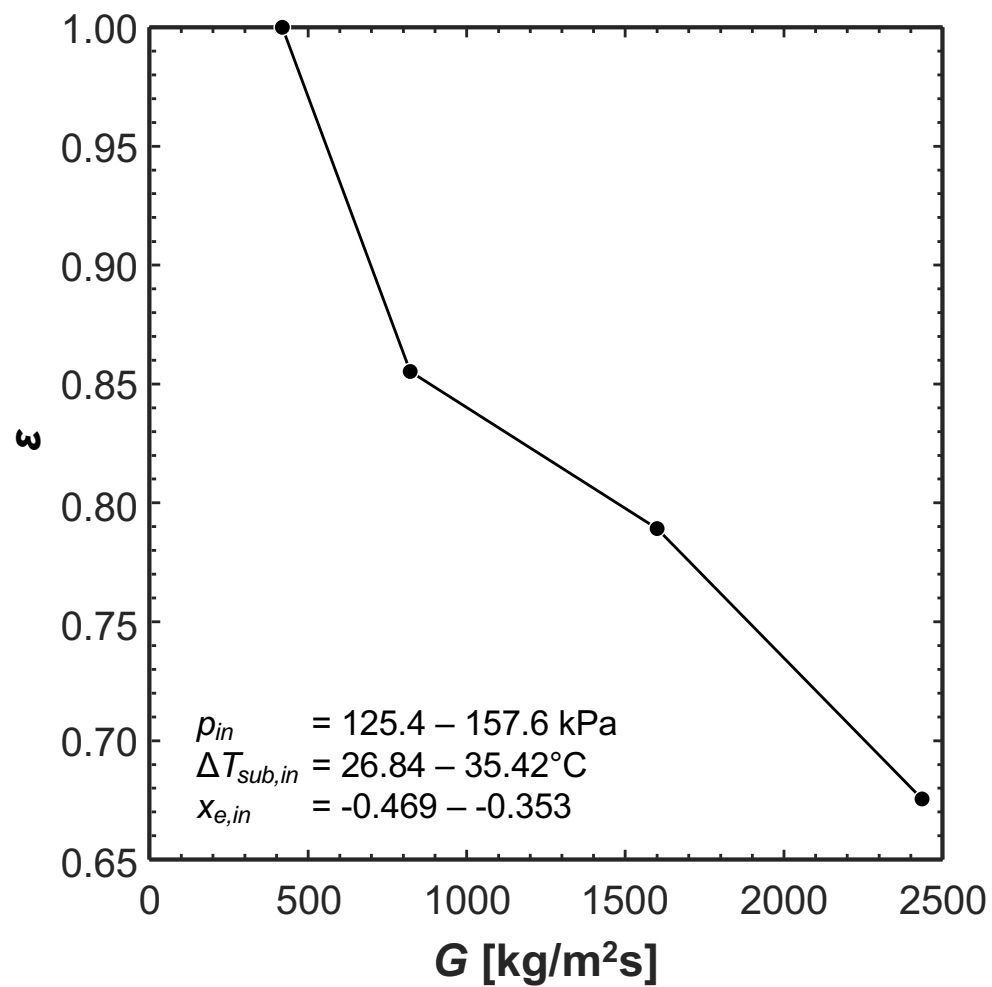
(a)

Modeled interface used in instability analysis

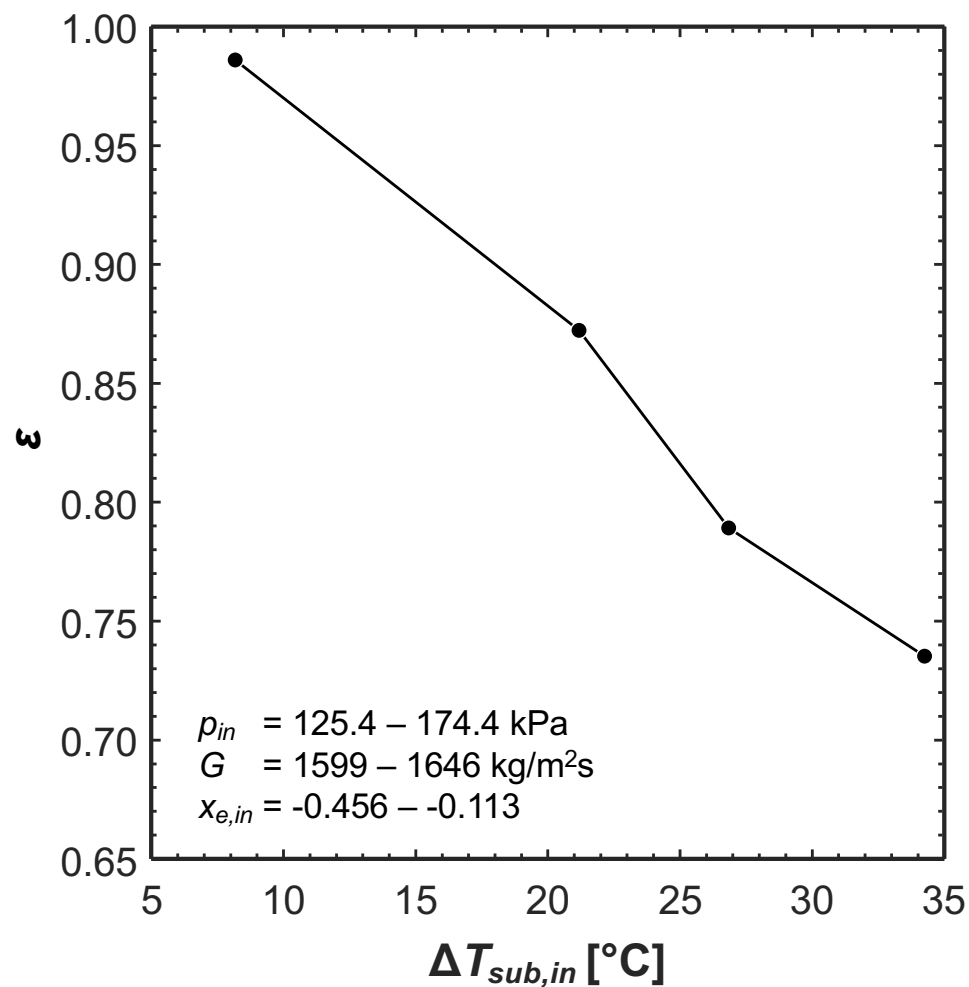


(b)

Fig. 11 Schematics of the (a) idealized formation of wavy liquid-vapor interface and (b) modeled interface used in instability analysis in a terrestrial environment.

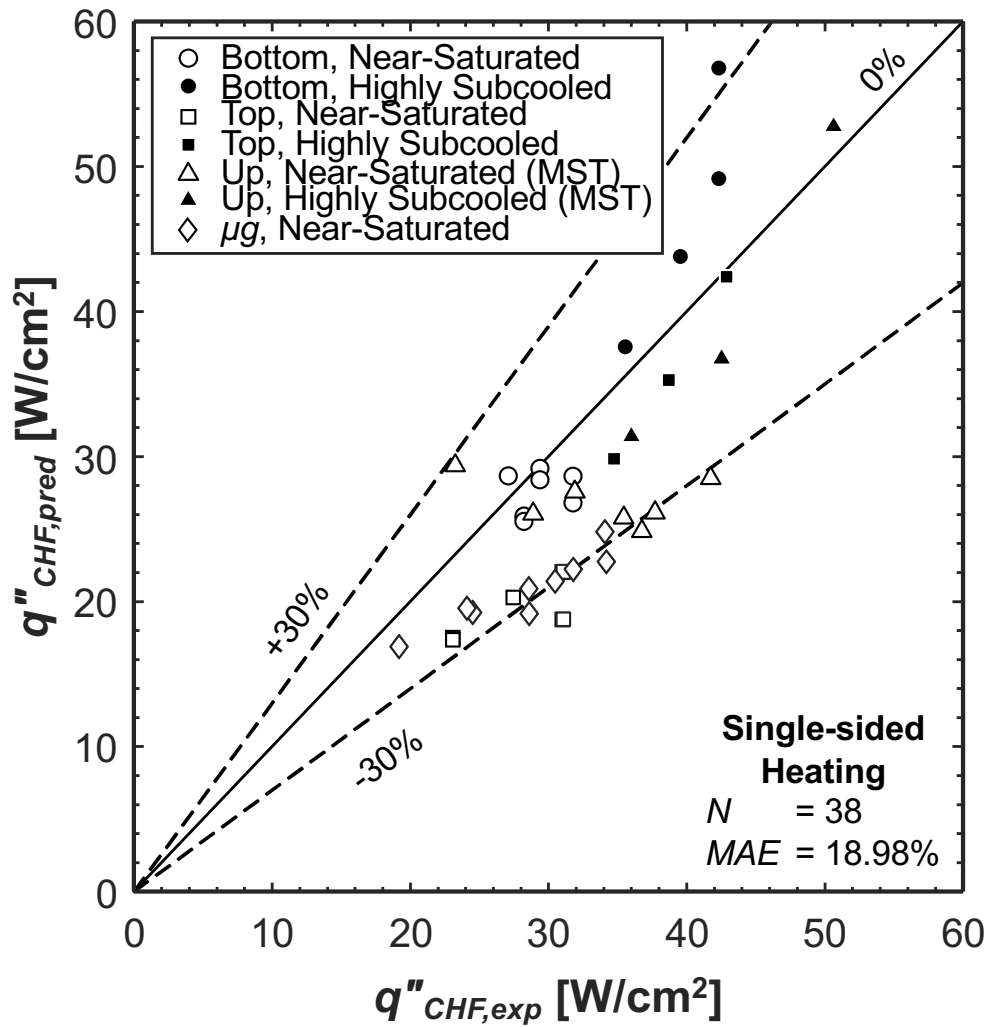


(a)

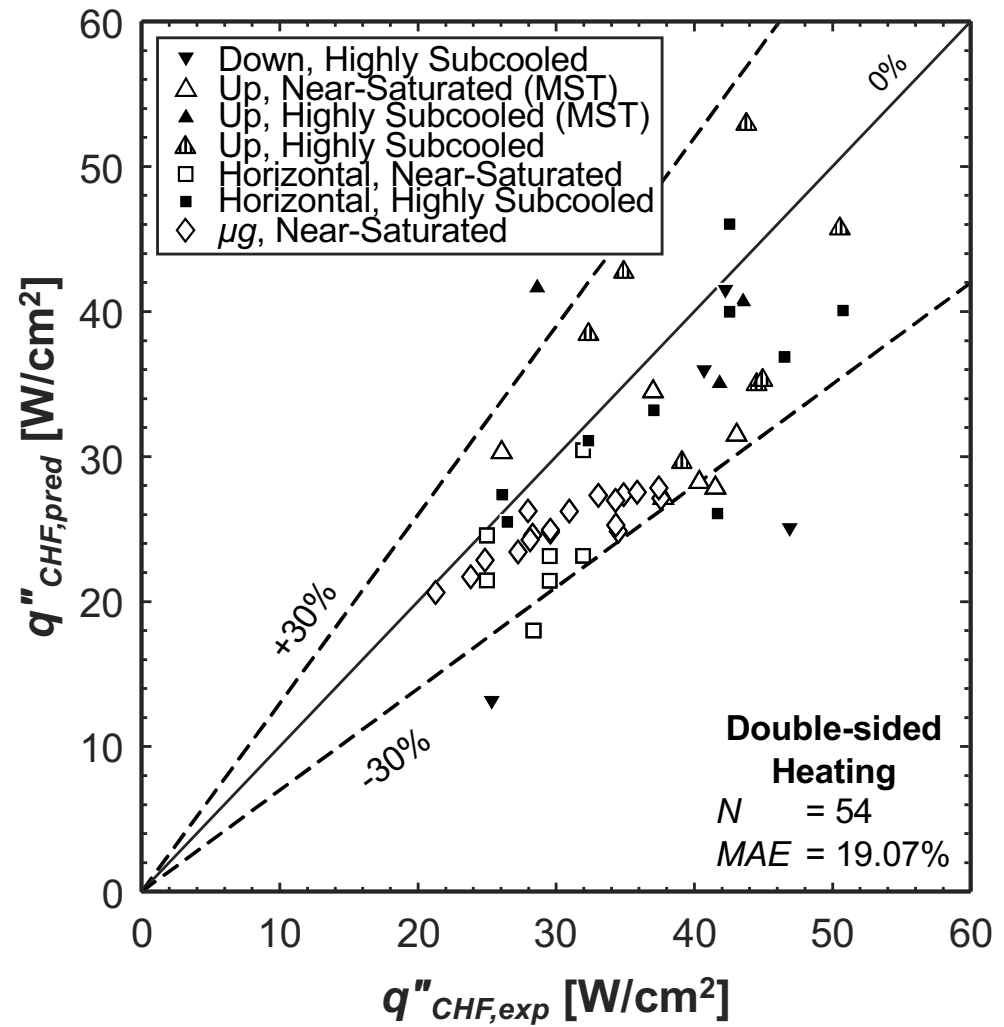


(b)

Fig. 12 Predicted heat utility ratio for different values of (a) mass velocity and (b) inlet subcooling.



(a)



(b)

Fig. 13 Comparison of experimental and predicted CHF values for (a) single-sided heating and (b) double-sided heating.